Superhydrophilic covalent organic frameworks accelerate photocatalytic production of hydrogen peroxide through proton channels

Xiaojuan Bai*[a,b], Linlong Guo[b], Tianqi Jia[b], Zhuofeng Hu*[c]

[a]Key Laboratory of Urban Stormwater System and Water Environment, Ministry of Education, Beijing University of Civil Engineering and Architecture, Beijing 100044, China

[b]Beijing Energy Conservation & Sustainable Urban and Rural Development Provincial and Ministry Co-construction Collaboration Innovation Center, Beijing University of Civil Engineering and Architecture, Beijing, China

[c]School of Environmental Science and Engineering, Guangdong Provincial Key Laboratory of Environmental Pollution Control and Remediation Technology, Sun Yat-sen University, Guangzhou, China

E-mail: baixiaojuan@bucea.edu.cn, heixia.1986@163.com

huzhf8@mail.sysu.edu.cn

S1. Experimental procedures

Chemicals and materials. Melamine, potassium iodide, potassium hydrogen phthalate, p−benzoquinone, disodium EDTA, tert−butanol, anhydrous ethanol, and hydrogen peroxide were purchased from Sinopharm Chemical Reagent Co, Ltd. 2,4,6−tris(4−aminophenyl)−1,3,5−triazine (TAPT), 1,4−Phthalaldehyde, terephthalaldehyde (PDA), tetrakis(4−aminophenyl)methane (TAPM), acetic acid, 1,3,5−trimethylbenzene, methanol, acetonitrile, dichloromethane and 1,2−dichlorobenzene were purchased from Shanghai Macklin Biochemical Co., Ltd. 2,5−dihydroxyterephthalaldehyde (DHA), ciprofloxacin, sulfamethoxazole, pyruvic acid, butanol and N−hexane were purchased from Aladdin Chemical Reagent Co. Ltd. All reagents purchased are analytical grade or above and can be used without further purification.

Synthesis of Melem: Melem was synthesized based on previous literature with slight modifications to the previous method. The melamine powder was placed in a covered crucible, after which the crucible was placed in a muffle furnace. The temperature of the muffle furnace was increased from 25 °C to 350 °C at a ramp rate of 10 °C min^{-1} and the muffle was kept at 350 °C and held for 2 h. After the temperature of the muffle furnace was cooled down to room temperature, the crucible was removed and the white product was obtained.

Synthesis of Melem−PDA: A certain amount of Melem (13.1 mg) and 1,4−Phthalaldehyde (PDA) (12.1 mg) were taken into a 25 mL glass beaker. Then 4 mL of 1,3,5−trimethylbenzene and 8 mL of aqueous 6 M acetic acid were added and sonicated for 20 min for uniform dispersion. The mixed solution was transferred to a polytetrafluoroethylene liner, and a series of COFs were obtained after microwave irradiation at 100 ℃, 120 ℃, and 150 ℃ for 1 h and 2 h, respectively. After cooling to room temperature, the solids were washed with a large amount of dichloromethane

(3 × 30 mL) and methanol (3 × 30 mL) in turn. Finally, the sample COF−TAPT/PDA was dried in a vacuum oven at 100 ℃ for 8 h to obtain the sample Melem−PDA.

Synthesis of TAPT−PDA: A certain amount of TAPT (21.3 mg) and PDA (12.1 mg) were taken into a 25 mL glass beaker. Then 4 mL of 1,3,5−trimethylbenzene and 8 mL of aqueous 6 M acetic acid were added and sonicated for 20 min for uniform dispersion. The mixed solution was transferred to a polytetrafluoroethylene liner, and a series of COFs were obtained after microwave irradiation at 100 ℃, 120 ℃, and 150 ℃ for 1 h and 2 h, respectively. After cooling to room temperature, the solids were washed with a large amount of dichloromethane (3 × 30 mL) and methanol (3 × 30 mL) in turn. Finally, the sample TAPT−PDA was dried in a vacuum oven at 100 ℃ for 8 h to obtain the sample TAPT−PDA.

Synthesis of TAPM−PDA: A certain amount of TAPM (22.8 mg) and PDA (12.1 mg) were taken into a 25 mL glass beaker. Then 4 mL of 1,3,5−trimethylbenzene and 8 mL of aqueous 6 M acetic acid were added and sonicated for 20 min for uniform dispersion. The mixed solution was transferred to a polytetrafluoroethylene liner, and a series of COFs were obtained after microwave irradiation at 100 ℃, 120 ℃, and 150 ℃ for 1 h and 2 h, respectively. After cooling to room temperature, the solids were washed with a large amount of dichloromethane (3 × 30 mL) and methanol (3 × 30 mL) in turn. Finally, the COF−TAPM/PDA was dried in a vacuum oven at 100 °C for 8 h to obtain TAPM−PDA.

Synthesis of Melem−DHA: An amount of Melem (13.1 mg) and DHA (15.0 mg) was taken into a 25 mL glass beaker. Then 4 mL of 1,3,5−trimethylbenzene and 8 mL of aqueous 6 M acetic acid were added and sonicated for 20 min for uniform dispersion. The mixed solution was transferred to a polytetrafluoroethylene liner, and a series of COFs were obtained after microwave irradiation at 100 ℃, 120 ℃, and 150 ℃ for 1 h and 2 h, respectively. After cooling to room temperature, the solids were washed with a large amount of dichloromethane (3 × 30 ml) and methanol (3 × 30 ml) in turn.

Finally, the sample Melem−DHA was dried in a vacuum oven at 100 ℃ for 8 h to obtain the sample Melem−DHA.

Synthesis of TAPT−DHA: A certain amount of TAPT (13.1 mg) and DHA (15.0 mg) were taken into a 25 mL glass beaker. Then 4 mL of 1,3,5−trimethylbenzene and 8 mL of aqueous 6 M acetic acid were added and sonicated for 20 min for uniform dispersion. The mixed solution was transferred to a polytetrafluoroethylene liner, and a series of COFs were obtained after microwave irradiation at 100 ℃, 120 ℃, and 150 ℃ for 1 h and 2 h, respectively. After cooling to room temperature, the solids were washed with a large amount of dichloromethane (3 × 30 mL) and methanol (3 × 30 mL) in turn. Finally, the samples were dried in a vacuum oven at 100 ℃ for 8 h to obtain the sample TAPT−DHA.

Synthesis of TAPM−DHA: A certain amount of TAPM (22.8 mg) and DHA (15.0 mg) were taken into a 25 mL glass beaker. Then 4 mL of 1,3,5−trimethylbenzene and 8 mL of aqueous 6 M acetic acid were added and sonicated for 20 min for uniform dispersion. The mixed solution was transferred to a polytetrafluoroethylene liner, and a series of COFs were obtained after microwave irradiation at 100 ℃, 120 ℃, and 150 ℃ for 1 h and 2 h, respectively. After cooling to room temperature, the solids were washed with a large amount of dichloromethane (3 × 30 mL) and methanol (3 × 30 mL) in turn. Finally, the samples were dried in a vacuum oven at 100 ℃ for 8 h to obtain the sample TAPM−DHA.

S2. Supporting Figures and Tables

Different COFs material precursors (Melem, TAPT, TAPM, PDA, DHA) were selected for microwave synthesis under different conditions (temperature for 100 ℃, 120 ℃, 150 ℃, time for 1 h, 2 h), and the synthesized routes are shown in **Figure S1** below, and a total of 36 samples were synthesized from A1 labeling to F6, respectively, with the specific precursors and conditions as shown in **Table S1** and the photocatalytic production of H_2O_2 was tested after the synthesis of COFs materials. As can be seen from **Figure S2** and **Figure S3**, the H_2O_2 yields of the synthesized samples under microwave treatment at 120 °C for 1 h were higher, and the TAPT−DHA series of samples had the best performance, with the highest photocatalytic H_2O_2 yield of up to 1629 $\mu mol \cdot h^{-1} \cdot g^{-1}$ for the highest D3 sample (TAPT−DHA).

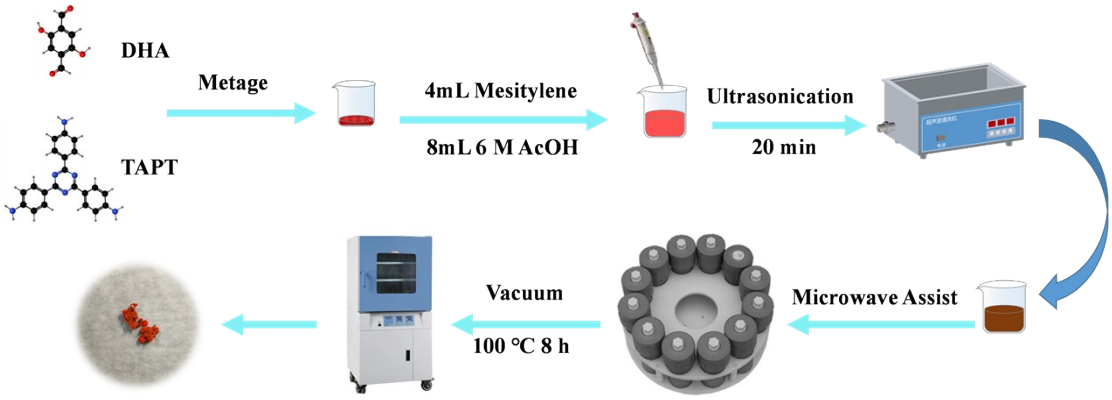

Figure S1. Sample synthesis process.

Table S1. Synthesis of samples.

Samples		Melem		TAPT		TAPM	
		1 h	2 h	1 h	2 h	1 h	2 h
PDA	100 ℃	A1	A2	C1	C2	E1	E2
	120 ℃	A3	A4	C3	C4	E3	E4
	150 ℃	A5	A6	C5	C6	E5	E6
DHA	100 ℃	B1	B2	D1	D2	F1	F2
	120 ℃	B3	B4	D3	D4	F3	F4
	150 ℃	B5	B6	D5	D6	F5	F6

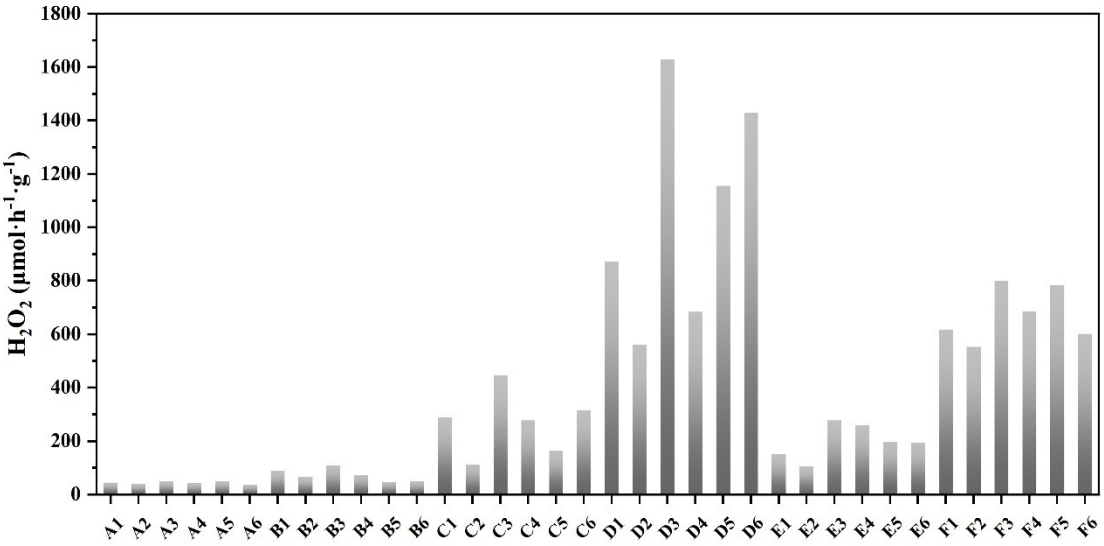

Figure S2. Comparison of photocatalytic H_2O_2 production performance of COFs samples.

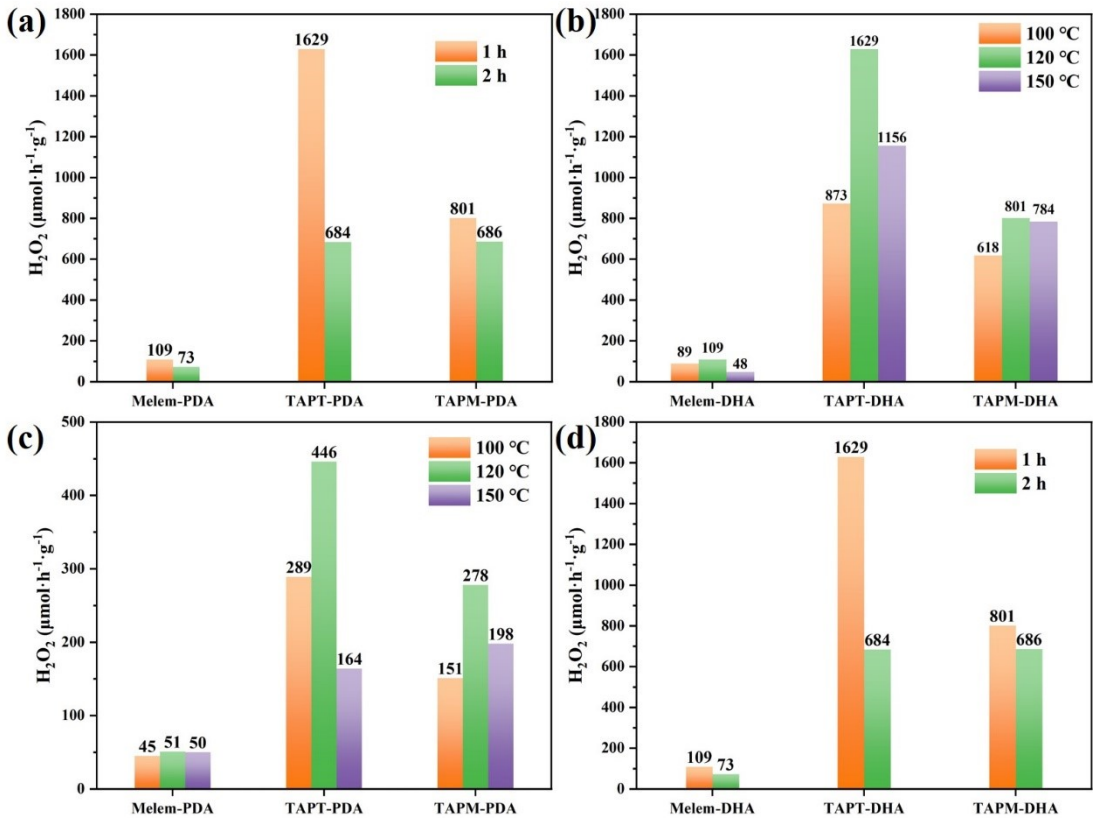

Figure S3. Comparison of H_2O_2 production performance of COFs under different synthesis conditions.

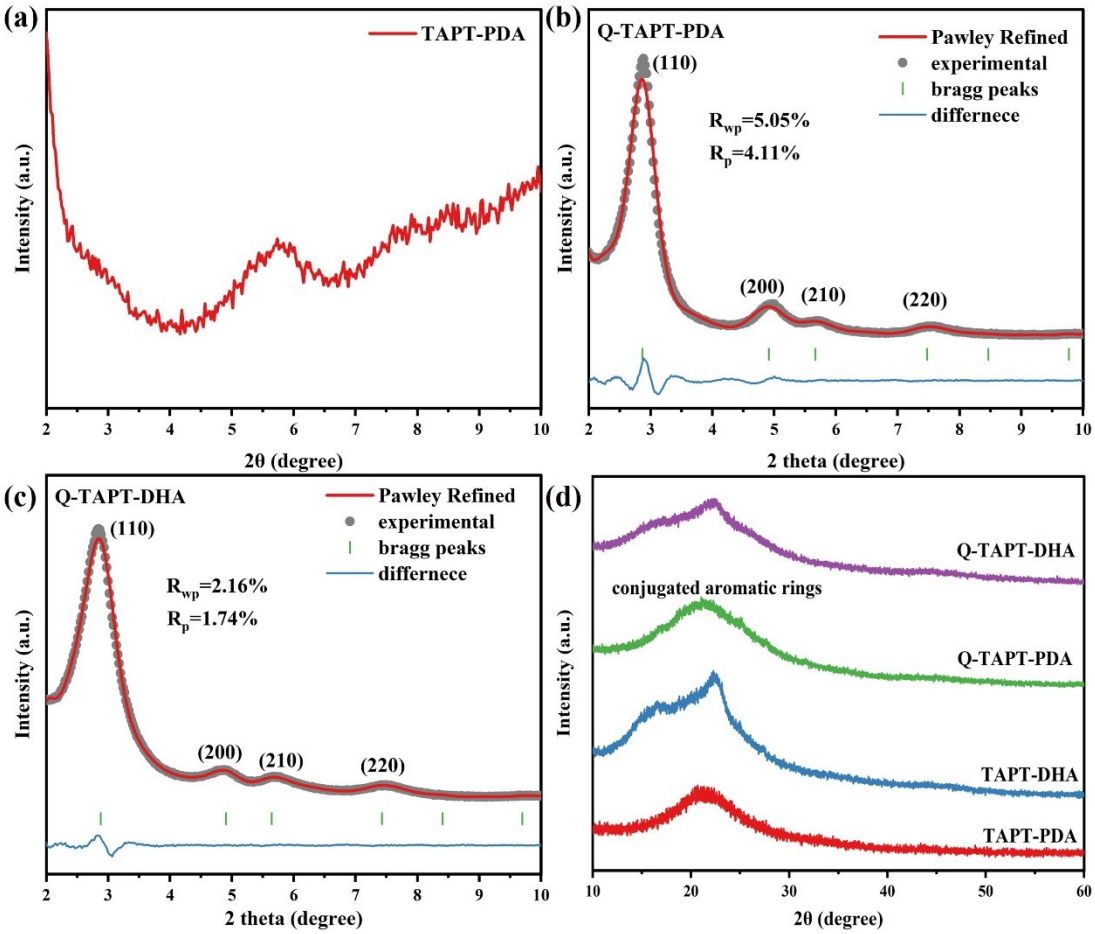

Figure S4. XRD patterns of TAPT−PDA, Q−TAPT−PDA and Q−TAPT−DHA.

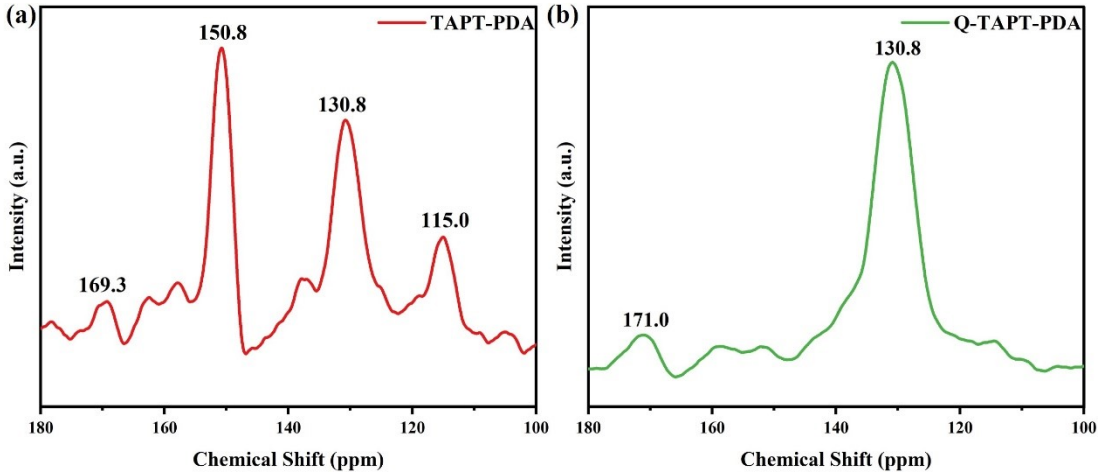

Figure S5. Solid−state ^{13}C CP−MAS NMR spectra of TAPT−PDA and Q−TAPT−PDA.

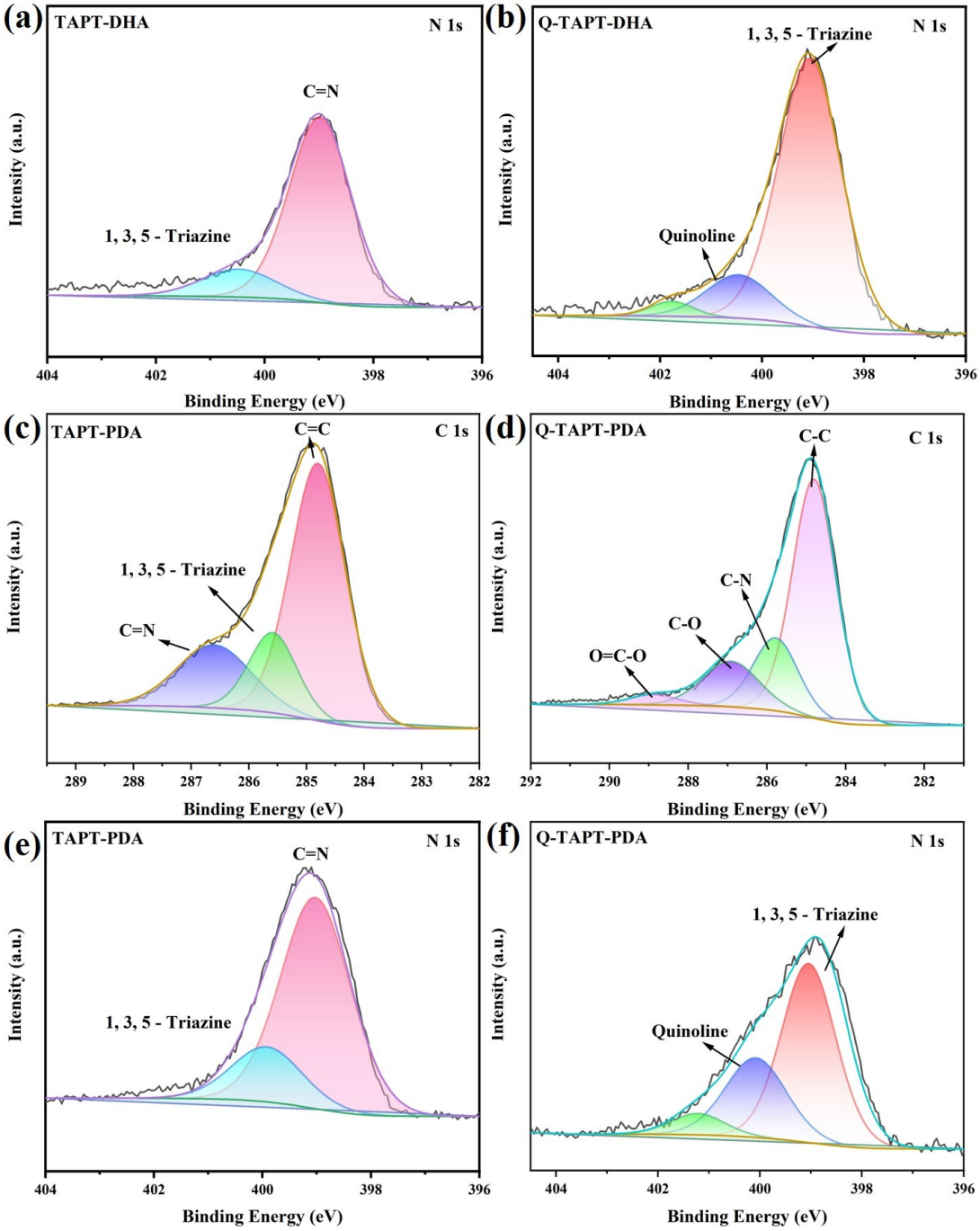

Figure S6. N 1s spectrum of (a) TAPT−DHA, (b) Q−TAPT−DHA, (d) TAPT−PDA and (e) Q−TAPT−PDA. C 1s spectrum of (c) TAPT−PDA and (d) Q−TAPT−PDA.

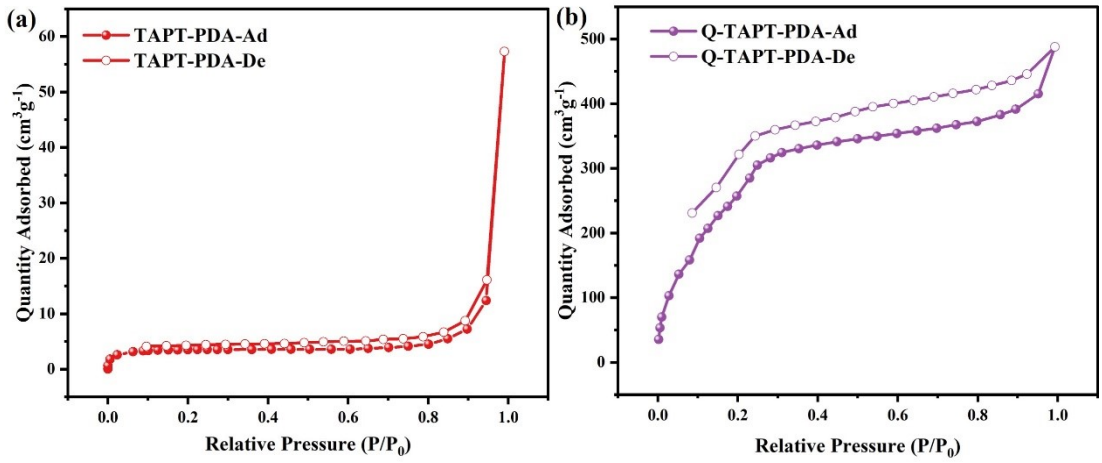

Figure S7. N_2 adsorption and desorption curves of TAPT−PDA and Q−TAPT−PDA.

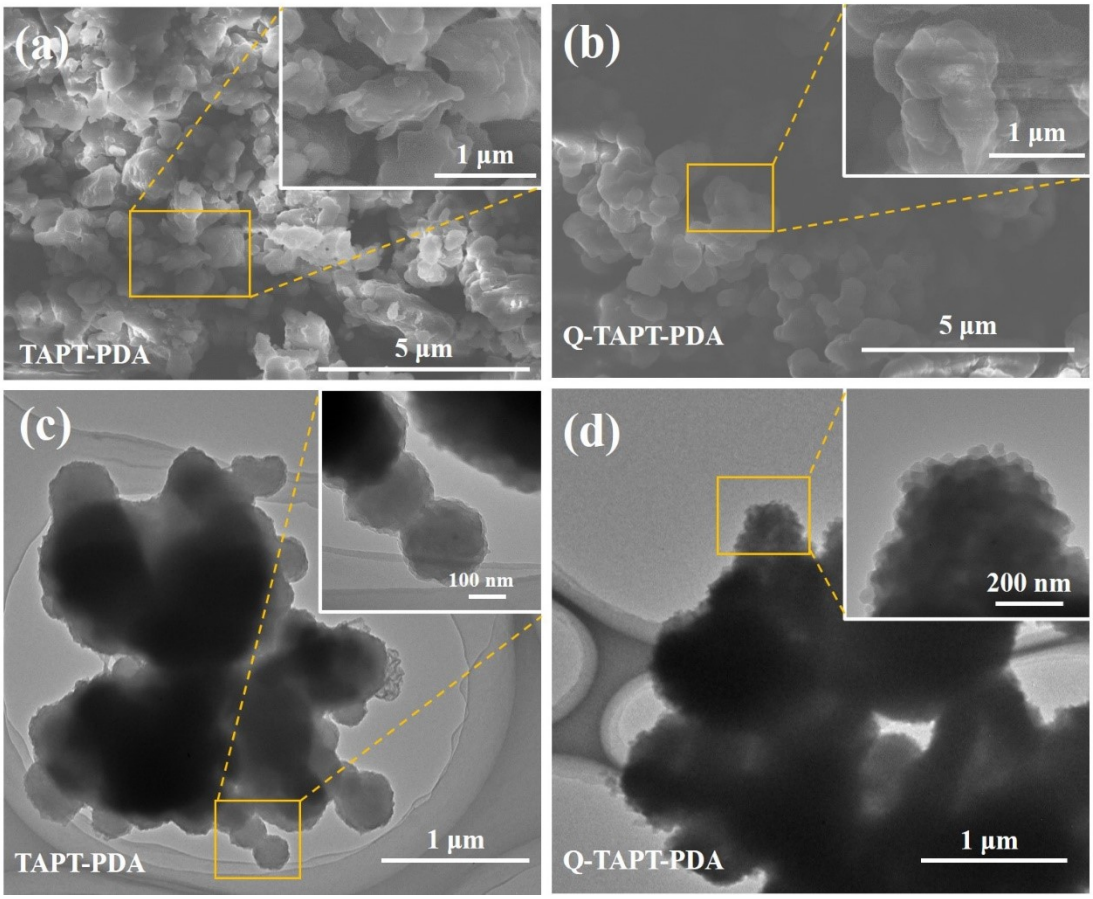

Figure S8. SEM image of (a) TAPT−PDA and (b) Q−TAPT−PDA at a scale of 5 µm. TEM image of (c) TAPT−PDA and (d) Q−TAPT−PDA at a scale of 1 µm.

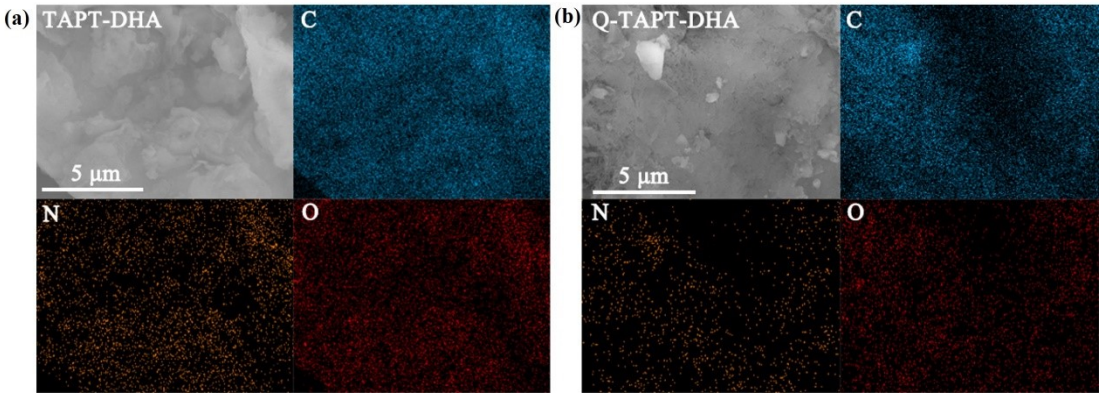

Figure S9. EDX mapping images of C, N and O elements in TAPT−DHA and Q−TAPT−DHA.

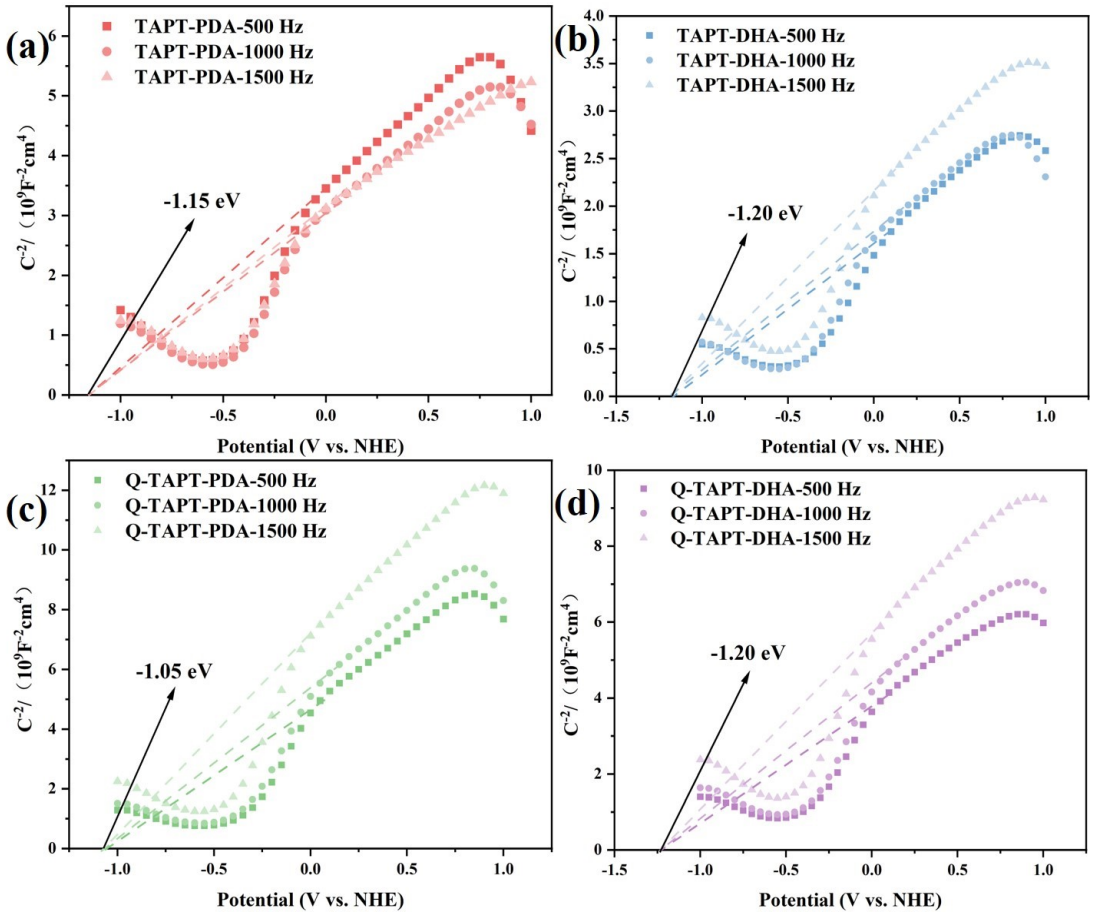

Figure S10. Mott−Schottky plots of (a) TAPT−PDA, (b) TAPT−DHA, (c) Q−TAPT−PDA and (d) Q−TAPT−DHA at frequencies of 0.5, 1.0, and 1.5 kHz.

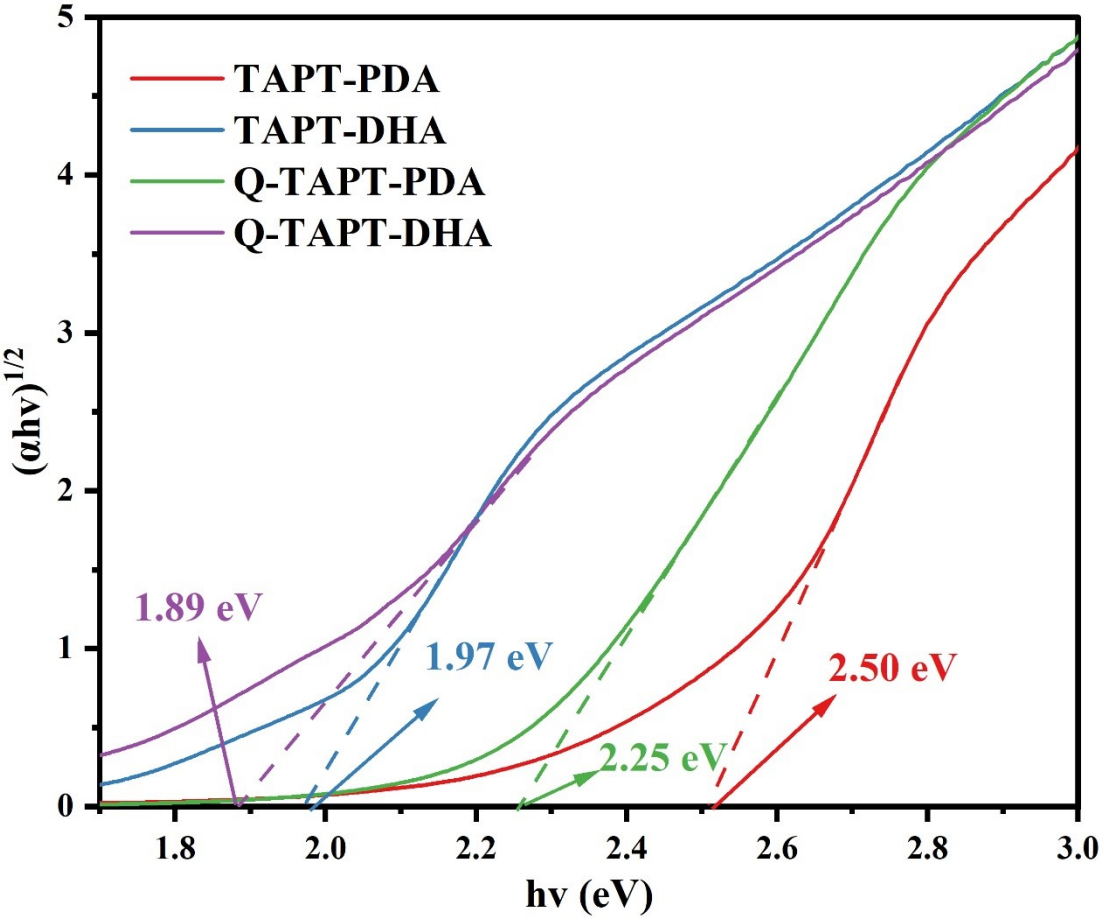

Figure S11. The energy gap of TAPT−PDA, TAPT−DHA, Q−TAPT−PDA and Q−TAPT−DHA that were estimated by the Tauc plot.

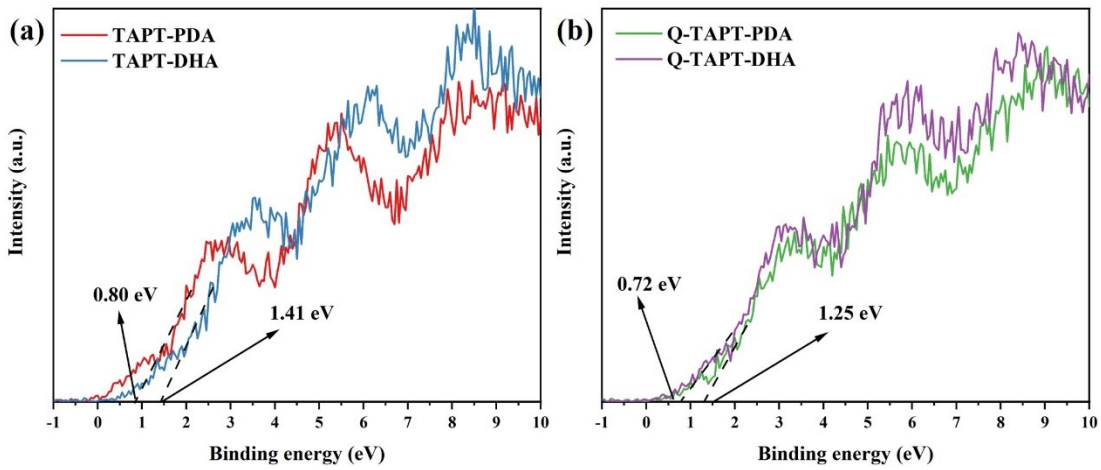

Figure S12. XPS VB spectrum of (a) TAPT−PDA, TAPT−DHA, (b) Q−TAPT−PDA and Q−TAPT−DHA.

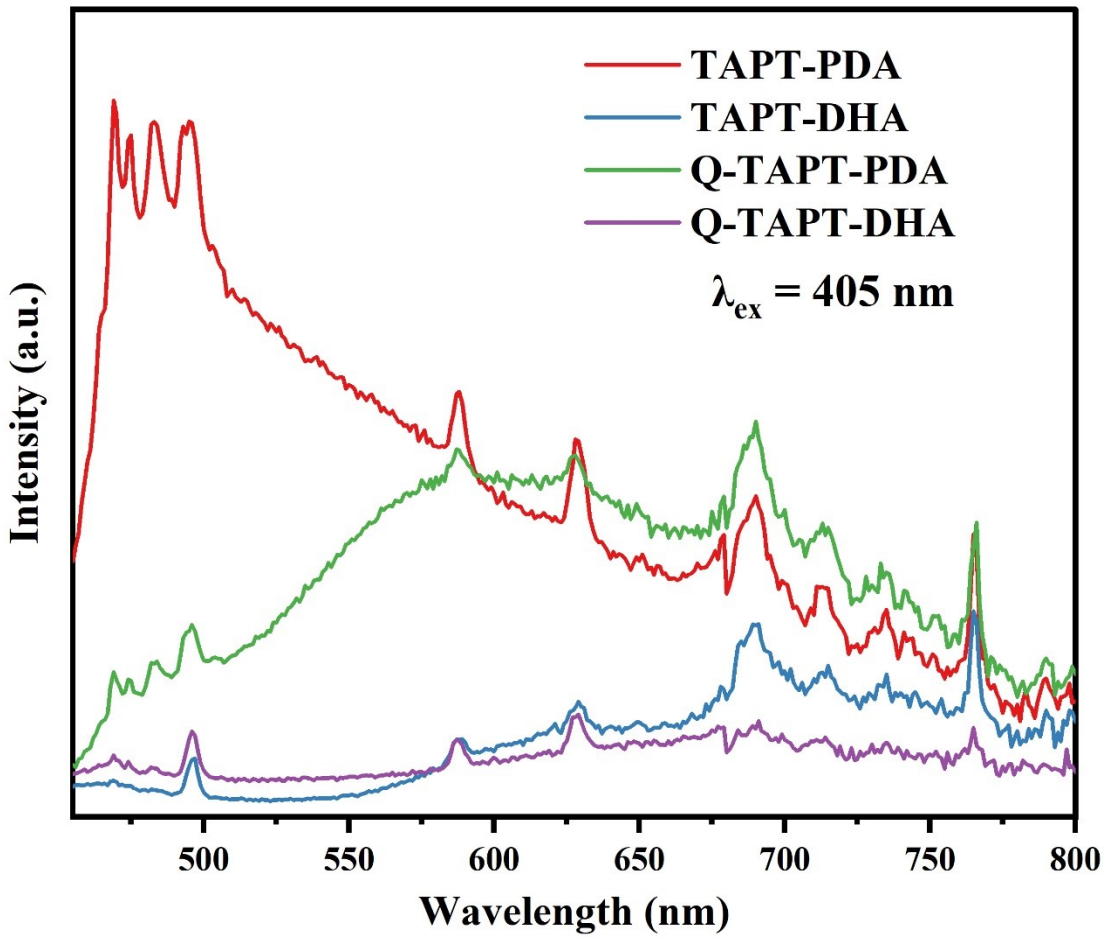

Figure S13. PL spectra of TAPT−PDA, TAPT−DHA, Q−TAPT−PDA and Q−TAPT−DHA, with the excitation wavelength of 405 nm.

Table S2 Comparison of recent photocatalytic performance of H_2O_2 produced by other COFs materials

Samples	Solution	Atmosphere	Light source	H_2O_2 generation rate ($\mu mol \cdot g^{-1} \cdot h^{-1}$)	AQY (%) (@420 nm)	Ref.
TAPD−$(Me)_2$COF	10% EtOH	O_2	420−700 nm	97	/	[1]
sonoCOF−F2	H_2O	Air	AM 1.5	1244.44	4.8%	[2]
COF−TTA−TTTA	H_2O	O_2	>420 nm	2406	/	[3]
TAPB−PDA−OH	10% EtOH	O_2	>420 nm	2117.6	2.99%	[4]
COF−TfpBpy	H_2O	Air	420−700 nm	694.7	8.1%	[5]
CoPc−BTM−COF	10% EtOH	O_2	>400 nm	2096	7.2% at 630 nm	[6]
DETH−COF	H_2O	Air	≥420 nm	1665	0.063% at 450 nm	[7]
4PE−N−S COF	H_2O	O_2	420−700 nm	1574	/	[8]
DMCR−1NH	H_2O	Air	>420 nm	2264.5	10.2%	[9]
PyDa−COF	50% BA	O_2	420−700 nm	1223.3	4.5%	[10]
1H−COF	10% IPA	O_2	>420 nm	1483.3	5.4%	[11]
TpAQ−COF−12	H_2O	O_2	>420 nm	420	7.4%	[12]
Bpy−TAPT	H_2O	O_2	>420 nm	4038	8.6%	[13]
CHF−DPDA	H_2O	O_2	>420 nm	1725	16%	[14]
HEP−TAPT−COF	H_2O	O_2	>420 nm	1750	15.35%	[15]
TiCOF−spn	90% EtOH	O_2	420−780 nm	489.94	/	[16]
COF−NUST−16	10% EtOH	O_2	>420 nm	1081	5.1% at 400 nm	[17]
ZnO/COF	10% EtOH	O_2	AM1.5	2443	13.12% at 365 nm	[18]
TiO_2/BTTA	Furfuyl alcohol	O_2	350−780 nm	740	/	[19]
TAPT−DHA	**H_2O**	**Air**	**AM1.5**	**1629**	**6.52% 7.79% at**	**This work**

					450 nm	
Q−TAPT−DHA	**H_2O**	**Air**	**AM1.5**	**1547**	**/**	**This work**

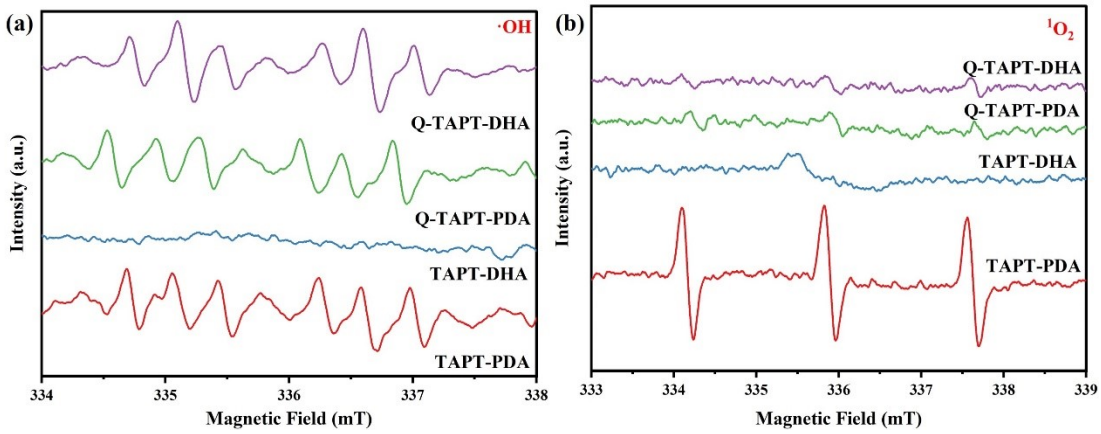

Figure S14. ESR spectra of ·OH and $^1O_2$ of TAPT−PDA, TAPT−DHA, Q−TAPT−PDA and Q−TAPT−DHA.

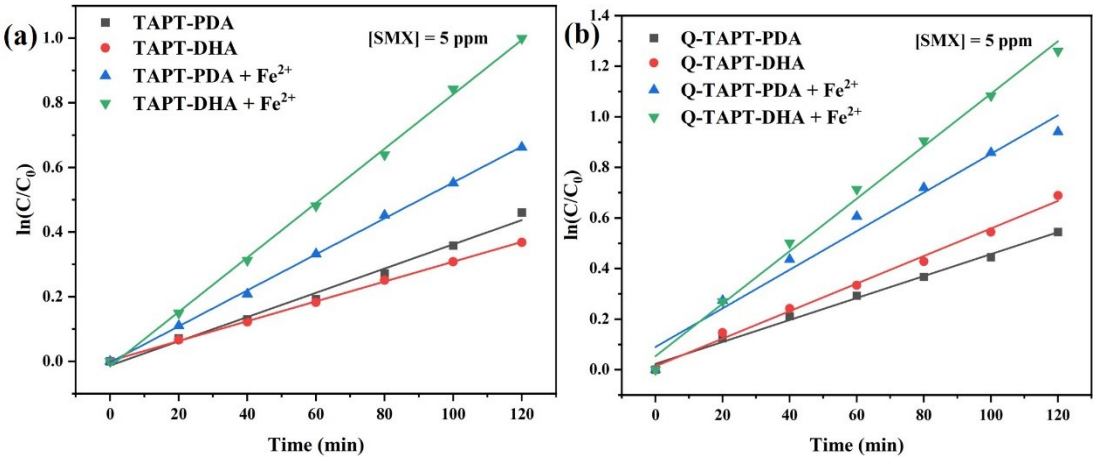

Figure S15. The first order kinetic constants of SMX degradation.

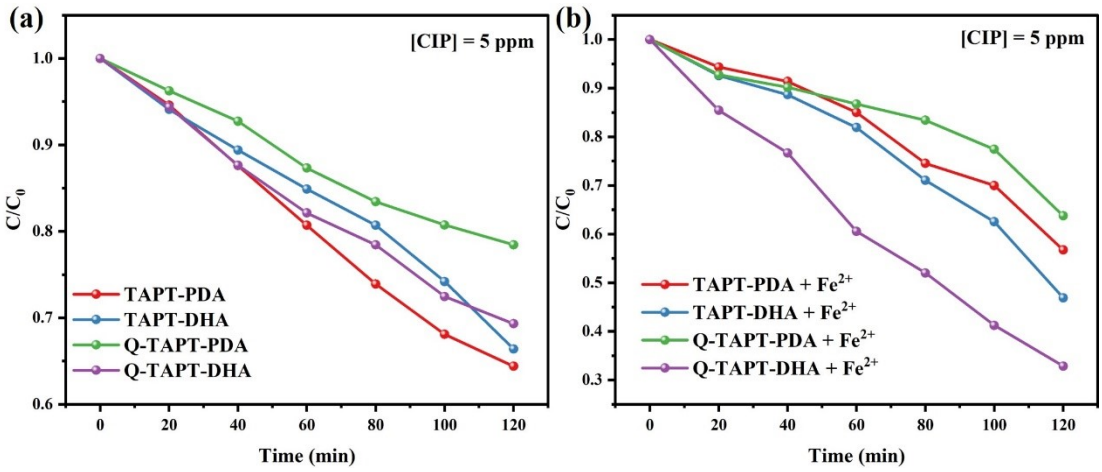

Figure S16. (a) Photocatalytic degradation of CIP by TAPT−PDA, TAPT−DHA, Q−TAPT−PDA and Q−TAPT−DHA. (b) Photocatalytic self−Fenton degradation of CIP by TAPT−PDA, TAPT−DHA, Q−TAPT−PDA and Q−TAPT−DHA.

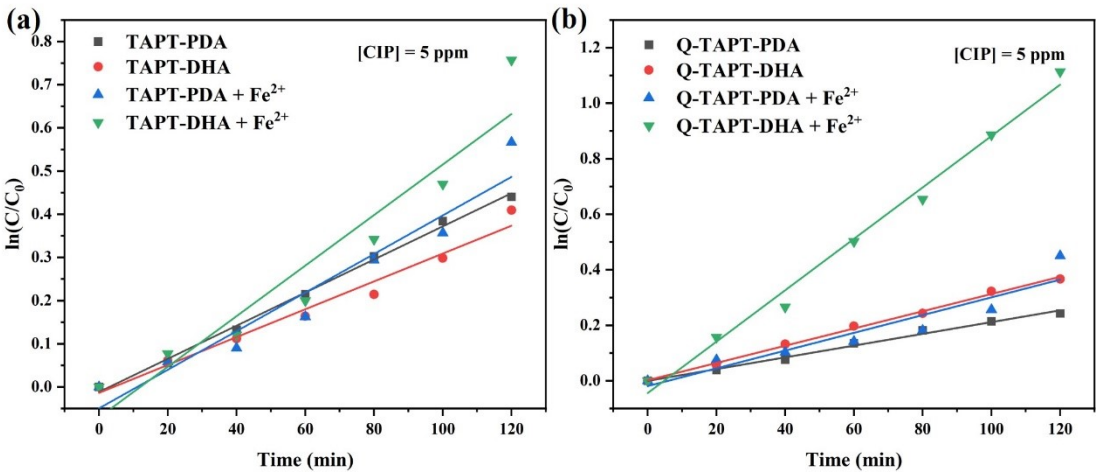

Figure S17. The first order kinetic constants of CIP degradation.

References

[1] C. Krishnaraj, H. Sekhar Jena, L. Bourda, A. Laemont, P. Pachfule, J. r. m. Roeser, C. V. Chandran, S. Borgmans, S. M. Rogge, K. Leus, *J. Am. Chem. Soc.* **2020**, *142*, 20107-20116.

[2] W. Zhao, P. Yan, B. Li, M. Bahri, L. Liu, X. Zhou, R. Clowes, N. D. Browning, Y. Wu, J. W. Ward, *J. Am. Chem. Soc.* **2022**, *144*, 9902-9909.

[3] F. Tan, Y. Zheng, Z. Zhou, H. Wang, X. Dong, J. Yang, Z. Ou, H. Qi, W. Liu, Z. Zheng, *CCS Chemistry* **2022**, *4*, 3751-3761.

[4] Y. Yang, J. Kang, Y. Li, J. Liang, J. Liang, L. Jiang, D. Chen, J. He, Y. Chen, J. Wang, *New. J. Chem.* **2022**, *46*, 21605-21614.

[5] M. Kou, Y. Wang, Y. Xu, L. Ye, Y. Huang, B. Jia, H. Li, J. Ren, Y. Deng, J. Chen, *Angew. Chem. Int. Ed.* **2022**, *61*, e202200413.

[6] Q. Zhi, W. Liu, R. Jiang, X. Zhan, Y. Jin, X. Chen, X. Yang, K. Wang, W. Cao, D. Qi, *J. Am. Chem. Soc.* **2022**, *144*, 21328-21336.

[7] G. Pan, X. Hou, Z. Liu, C. Yang, J. Long, G. Huang, J. Bi, Y. Yu, L. Li, *ACS Catal.* **2022**, *12*, 14911-14917.

[8] M. Deng, J. Sun, A. Laemont, C. Liu, L. Wang, L. Bourda, J. Chakraborty, K. Van Hecke, R. Morent, N. De Geyter, *Green. Chem.* **2023**, *25*, 3069-3076.

[9] P. Das, G. Chakraborty, J. Roeser, S. Vogl, J. Rabeah, A. Thomas, *J. Am. Chem. Soc.* **2023**, *145*, 2975-2984.

[10] J. Sun, H. Sekhar Jena, C. Krishnaraj, K. Singh Rawat, S. Abednatanzi, J. Chakraborty, A. Laemont, W. Liu, H. Chen, Y. Y. Liu, *Angew. Chem. Int. Ed.* **2023**, *62*, e202216719.

[11] H. Hu, Y. Tao, D. Wang, C. Li, Q. Jiang, Y. Shi, J. Wang, J. Qin, S. Zhou, Y. Kong, *J. Colloid. Interf. Sci.* **2023**, *629*, 750-762.

[12] X. Zhang, J. Zhang, J. Miao, X. Wen, C. Chen, B. Zhou, M. Long, *Chem. Eng. J.* **2023**, *466*, 143085.

[13] Y. Liu, W.-K. Han, W. Chi, Y. Mao, Y. Jiang, X. Yan, Z.-G. Gu, *Appl. Catal. B* **2023**, *331*, 122691.

[14] H. Cheng, H. Lv, J. Cheng, L. Wang, X. Wu, H. Xu, *Adv. Mater.* **2022**, *34*,

2107480.

[15] D. Chen, W. Chen, Y. Wu, L. Wang, X. Wu, H. Xu, L. Chen, *Angew. Chem. Int. Ed.* **2023**, *135*, e202217479.

[16] W.-K. Han, H.-S. Lu, J.-X. Fu, X. Liu, X. Zhu, X. Yan, J. Zhang, Y. Jiang, H. Dong, Z.-G. Gu, *Chem. Eng. J.* **2022**, *449*, 137802.

[17] M. Wu, Z. Shan, J. Wang, T. Liu, G. Zhang, *Chem. Eng. J.* **2023**, *454*, 140121.

[18] Y. Zhang, J. Qiu, B. Zhu, M. Fedin, B. Cheng, J. Yu, L. Zhang, *Chem. Eng. J.* **2022**, *444*, 136584.

[19] Y. Yang, J. Liu, M. Gu, B. Cheng, L. Wang, J. Yu, *Appl. Catal. B* **2023**, *333*, 122780.